

## Electronic Supplementary information (ESI)

### The effect of branching in a semiconducting polymer on the efficiency of organic photovoltaic cells

Gaël H. L. Heintges,<sup>†</sup> Jacobus J. van Franeker,<sup>†,‡</sup> Martijn M. Wienk,<sup>†,§</sup> and René A. J. Janssen<sup>\*,†,§</sup>

<sup>†</sup>Molecular Materials and Nanosystems & Institute for Complex Molecular Systems, Eindhoven University of Technology, P.O. Box 513, 5600 MB Eindhoven, The Netherlands

<sup>‡</sup>Dutch Polymer Institute (DPI), P.O. Box 902, 5600 AX Eindhoven, The Netherlands

<sup>§</sup>Dutch Institute for Fundamental Energy Research, De Zaale 20, 5612 AJ Eindhoven, The Netherlands

#### 1. Synthesis

##### General method and materials

Commercial solvents and reactants were used as received unless stated otherwise. [70]PCBM (purity 90-95%) was purchased from Solenne BV. 3,6-bis(5-bromothiophen-2-yl)-2,5-bis(2-decyltetradecyl)-2,5-dihydropyrrolo[3,4-c]pyrrole-1,4-dione was synthesized according to literature procedure.<sup>S1</sup> All other chemicals were purchased from Aldrich Chemical Co. 1,4-Bis(4,4,5,5-tetramethyl-1,3,2-dioxaborolan-2-yl)benzene and 1,3,5-tris(4,4,5,5-tetramethyl-1,3,2-dioxaborolan-2-yl)benzene were recrystallized from methanol prior to polymerization. DT-PDPPTPT was synthesized according to the previously published procedure.<sup>S1</sup>

##### 1B-DT-PDPPTPT

3,6-bis(5-bromothiophen-2-yl)-2,5-bis(2-decyltetradecyl)-2,5-dihydropyrrolo[3,4-c]pyrrole-1,4-dione (100 mg, 88.4  $\mu\text{mol}$ ), 1,4-Bis(4,4,5,5-tetramethyl-1,3,2-dioxaborolan-2-yl)benzene (28.7 mg, 87.1  $\mu\text{mol}$ ), 1,3,5-tris(4,4,5,5-tetramethyl-1,3,2-dioxaborolan-2-yl)benzene (0.40 mg, 0.88  $\mu\text{mol}$ ), triphenylphosphine (1.39 mg, 5.30  $\mu\text{mol}$ ) and tris(dibenzylideneacetone)dipalladium (1.21 mg, 1.331  $\mu\text{mol}$ ) were placed in a Schlenk-flask under argon. Dry toluene (2 ml) was added and the resulting solution was degassed with argon. A degassed aqueous 2M solution of tripotassium phosphate was subsequently added (0.22 ml) with a drop of aliquat 336 and the mixture was heated to 115°C. After reaction overnight, the crude product was dispersed in 1,1,2,2-tetrachloroethane (TCE) and subsequently poured into methanol. The filtered product was redissolved in TCE at 150°C. Ethylenediaminetetraacetic acid (200 mg) was added to this hot solution and stirred during one hour. Water was added, and the mixture was stirred vigorously for another hour at 110°C, after which the organic layer was separated, and washed with water. The polymer was then precipitated in methanol, and filtered in a soxhlet thimble. Soxhlet extraction using acetone, hexane, and dichloromethane was performed, after which the residue in the thimble was dissolved in hot TCE. This solution was subsequently precipitated in methanol and filtered, giving 1B-DT-PDPPTPT as a dark green solid.

## 2. Photovoltaic devices

### Fabrication

Photovoltaic devices with an active area of 0.09 and 0.16 cm<sup>2</sup> were fabricated on patterned indium tin oxide (ITO) glass substrates (Naranjo Substrates). Substrates were cleaned by sonication in acetone for 15 minutes, followed by scrubbing with a sodium dodecyl sulfate solution (99%, Acros), rinsing with deionized water and a final sonication step in 2-propanol. Finally, they underwent with UV-ozone treatment for 30 min. Poly(ethylenedioxythiophene):poly(styrenesulfonate) (PEDOT:PSS) (Clevios P, VP Al4083) was deposited via spin coating (3000 rpm, 40 nm), followed by the active layer. The polymers were dissolved at a concentration of 4 mg/ml together with [70]PCBM (8 mg/ml) in chloroform containing 3% or 6% of DIO by stirring one hour at 90°C. The solutions were cooled down to room temperature (stirring for 2 min.) prior to spin coating. The best devices were made using a spincoat speed of 1500 rpm, resulting in an active layer thickness of 104 nm in both cases. The back electrode, consisting of LiF (1 nm) and Al (100 nm), was deposited by evaporation under high vacuum ( $\sim 3 \times 10^{-7}$  mbar).

### Characterization

*JV* characteristics were measured with a Keithley 2400 source meter under ca. 100 mWcm<sup>-2</sup> white-light illumination from a tungsten–halogen lamp filtered by a Schott GG385 UV filter and a Hoya LB120 daylight filter. Short-circuit currents under AM 1.5G conditions were estimated by convoluting the spectral response with the solar spectrum. Spectral response measurements were conducted under 1 sun operating conditions by using a 532 nm solid state laser (Edmund Optics) for bias illumination. The device was kept in a nitrogen filled box behind a quartz window and irradiated with modulated monochromatic light, from a 50 W tungsten-halogen lamp (Philips focusline) and monochromator (Oriel, Cornerstone 130) with the use of a mechanical chopper. The modulated photocurrent was amplified with a Stanford Research System Model SR570 current preamplifier and then measured using a lock-in amplifier (Stanford research Systems SR830). A calibrated silicon cell was used as reference. TEM was performed on a Tecnai G 2 Sphera TEM (FEI) operated at 200 kV. Layer thicknesses were measured with a Veeco Dektak 150 profilometer.

### Internal quantum efficiency

The wavelength dependent index of refraction ( $n$ ) and extinction coefficient ( $k$ ) were obtained from the reflection and transmission of blend films of the optimized active layers on quartz (3 thicknesses) that were measured using a calibrated integrating sphere. Light absorption in the device stack was then modelled using Setfos 3.2 (Fluxim AG) software using the optical constants ( $n$ ,  $k$ ) of all layers in the stack and the transfer matrix formalism. By dividing the EQE with the fraction of photons absorbed by the active layer the internal quantum efficiency (IQE) was obtained at each wavelength (Fig. S1). The spectrally averaged IQE was found to be 51% in the case of DT-PDPPTPT and 71% in the case of 1B-DT-PDPPTPT. Hence, the increase in IQE represents 90% of the increase in spectrally averaged EQE, the other 10% being accounted for by the higher absorption of 1B-DT-PDPPTPT.

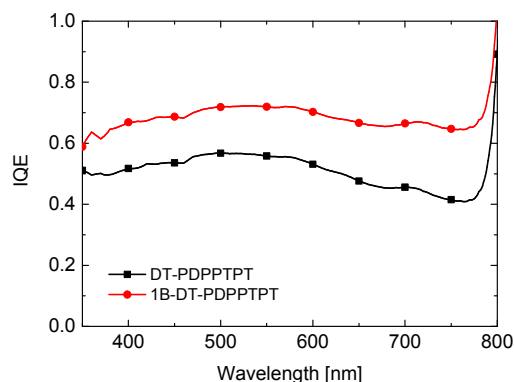


**Fig. S1.** Spectrally resolved internal quantum efficiency of the best device made with DT-PDPPTPT and 1B-DT-PDPPTPT.

### 3. Light scattering experiments

Silicon substrates (Si-Mat, 525  $\mu\text{m}$  thickness with 200 nm SiO<sub>2</sub> layer) were used, which were cleaned in the same way as the ITO substrates, but UV-ozone was replaced with an air plasma treatment (Diener Electronic Femto PCCE, 100% power, 10 minutes). A layer of poly(ethylenedioxythiophene):poly(styrene sulfonate) (PEDOT:PSS, Heraeus Clevis PVP Al 4083) was spin coated before the measurement, to ensure similar wetting properties as the ITO substrates. Simultaneously with the scattering experiments, solar cell devices were fabricated from the same solutions. All solar cells showed the same behaviour as before.

A Melles-Griot 5 mW HeNe laser (632.8 nm) was spread to a spot of  $\sim 3$  mm radius using a biconvex lens. The specular reflection (which contains the interference signal) from the spinning silicon substrate (1500 rpm) was diffused using white paper and collected with a Thor Labs SM1PD1A photodiode. A second photodiode (Hamamatsu S2281) collected light scattered by inhomogeneities in the spin-coating film. Both photodiodes were behind a Thor Labs FL632.8-3 laser line filter to remove unwanted environmental light from the signal. Two Stanford Research System Model SR570 current preamplifiers (high bandwidth mode, 10 nA V<sup>-1</sup>) amplified the signals, which were then recorded simultaneously with a time resolution of  $\sim 1$  ms by a Keithley 2636A sourcemeter.

The intensity of the specular reflected laser light is dependent on the interference of the light reflected from the top of the layer and the light reflected from the substrate. This intensity oscillates in time as the layer dries and the interference goes through maxima and minima as shown in Fig. S2. A script in Wolfram Mathematica 10.0 was used to select peaks and valleys in the interference signal, which were used to back-calculate the thickness evolution during solvent evaporation. Working backwards, each peak-valley adds a thickness of  $\sim 100$  nm ( $\lambda/(4n\cos\vartheta)$ ) to the layer thickness after chloroform evaporation, which is the final layer thickness and the remaining amount of DIO. The amount of DIO at that point is calculated using the volume ratio of DIO to solids in the initial spin coating solution.  $\lambda$  is the wavelength of the laser,  $\vartheta$  the

angle of incidence and the refractive index  $n$  was estimated using the approximate volume fractions of all components. Fig. 4a in the main text shows the layer thickness vs. time for the short times (about 1 s).

Fig. 4b shows the corresponding intensity of the scattered light that we attribute to the formation of fibres. To be able to directly compare the experiments, the curves were synchronized with respect to the last valley in the interference signal during the fast drying stage (Fig. S2). To demonstrate that drying of the layer continues after this fast drying stage (Fig. S2), two long measurements were performed, which indicate that the layer only dries completely after 1 to 1.5 hours (Fig. S3). This long drying time is related to the slow evaporation of DIO, which has a high boiling point. This indicates that only a very small amount of DIO will evaporate during the first 2 s of spin coating, which justifies the assumption made above that at point  $t = 0$  s the DIO content is the same as the initial DIO content.

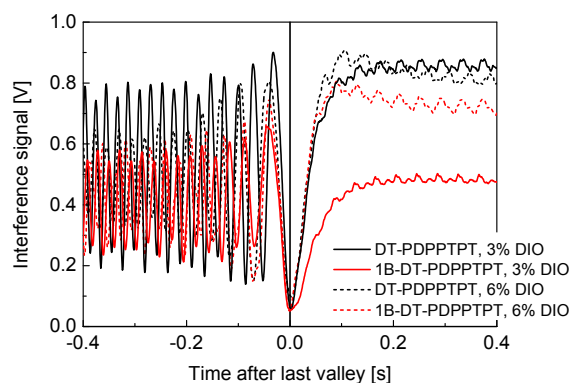


**Fig. S2.** Interference signal of the laser light during spin coating of the mixture of polymer, fullerene, solvent and co-solvent versus time. The signals of different experiments are manually synchronized at the last valley of the interference signal.

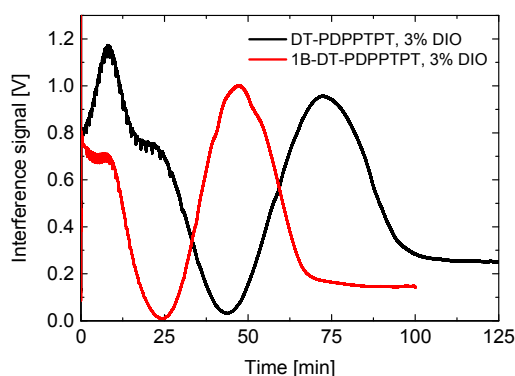


**Fig. S3.** Interference signals of laser light on the mixture of polymer, fullerene, solvent and co-solvent during spin coating versus time for the slow drying regime.

#### 4. Physical properties

Molecular-weight distributions of the polymers were estimated by GPC at 140 °C on a PL-GPC 120 system using a PL-GEL 10 mm MIXED-C column with *o*-DCB as the eluent and using polystyrene internal standards. Samples were dissolved in *o*-DCB at 140 °C for 2 hours and filtered hot through a heated 2  $\mu\text{m}$  PTFE filter. UV-vis-NIR spectroscopy was conducted on a PerkinElmer Lambda 900 or PerkinElmer Lambda 1050 spectrophotometer. Cyclic voltammetry was performed under an inert atmosphere with a scan speed of 0.1 V s<sup>-1</sup> on polymer films using a solution of 1 M tetrabutylammonium hexafluorophosphate in acetonitrile. A polymer-covered ITO substrate was used as the working electrode, a silver rod as counter electrode, and a silver rod coated with silver chloride (Ag/AgCl) as quasi-reference electrode in combination with Fc/Fc<sup>+</sup> as an internal standard.

#### 5. Additional graphs

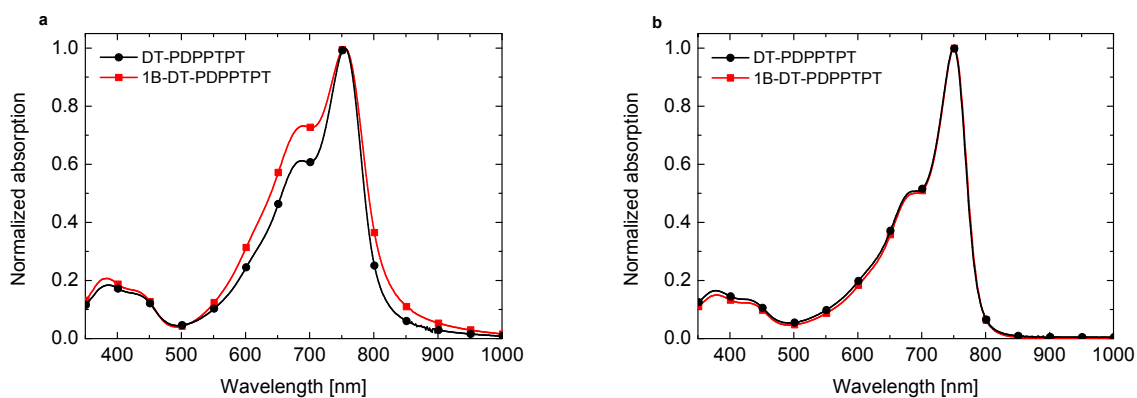


**Fig. S4.** UV-vis-NIR absorption of both polymers in film (a) and chloroform solution (b).

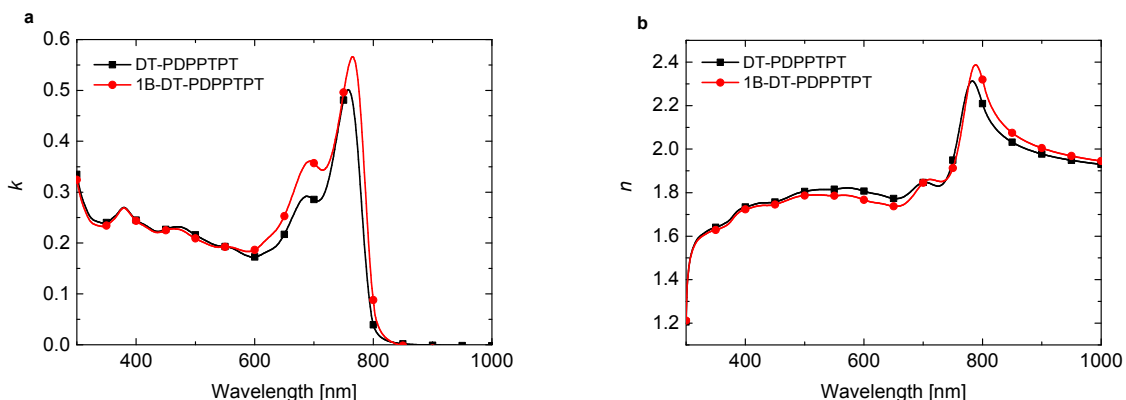


**Fig S5.**  $k$  (a) and  $n$  (b) for both materials in an optimized solar cell active layer blend.

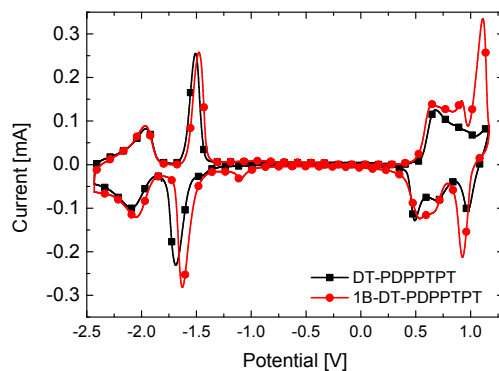


**Fig. S6.** Cyclic voltammetry of both polymer films recorded in acetonitrile, referenced versus  $Fc/Fc^+$ .

**Table S1.** GPC results of both polymers. Two measurements were performed on each polymer sample, to ensure that the result was reproducible. The values given in the main text are averages of the two measurements.

Polymer	$M_n$ [kDa] <sup>a</sup>	$M_w$ [kDa] <sup>b</sup>	PDI <sup>c</sup>	$M_p$ [kDa] <sup>d</sup>
DT-PDPPTPT	44.2	97.7	2.21	82.8
DT-PDPPTPT	46.5	102	2.20	87.1
1B-DT-PDPPTPT	33.0	112	3.38	43.9
1B-DT-PDPPTPT	29.8	105	3.53	42.2

<sup>a</sup> Number average molecular weight, <sup>b</sup> Weight average molecular weight, <sup>c</sup> Polydispersity, <sup>d</sup> Peak molecular weight.

## 6. Supplementary reference

- S1. W. Li, K. H. Hendriks, A. Furlan, W. S. C. Roelofs, M. M. Wienk, and R. A. J. Janssen, *Adv. Mater.* 2014, **26**, 1565–1570.